



Attachment of idarubicin to glutaraldehyde-coated magnetic nanoparticle and investigation of its effect in HL-60 cell line

Hasan ULUSAL^{1*}, Fatma ULUSAL², Mehmet Akif BOZDAYI¹, Bilgehan GÜZEL³,
Seyithan TAYSI¹, Mehmet TARAKÇIOĞLU¹

¹ Department of Medical Biochemistry, Faculty of Medicine, Gaziantep University, 27310, Gaziantep, Türkiye

² Department of Chemistry and Chemical Processing Technologies, Tarsus University, 33100, Mersin, Türkiye

³ Department of Chemistry, Faculty of Arts and Sciences, Cukurova University, 01330, Adana, Türkiye

Received: 26 October 2022; Revised: 1 November 2022; Accepted: 30 November 2022

* Corresponding author e-mail: hasan_ulusal@hotmail.com

Citation: Ulusal, H.; Ulusal, F.; Bozdayı, M. A.; Güzel, B.; Tayısı, S.; Tarakçıođlu, M. *Int. J. Chem. Technol.* 2022,6 (2), 154-163.

ABSTRACT

Idarubicin is a chemotherapeutic drug frequently used to treat breast cancer and acute leukemia. This study aimed to immobilize idarubicin on glutaraldehyde (GA)-coated magnetic nanoparticles (MNP-GA) to prepare a drug with high stability and low toxicity. We preferred MNPS because of their easy synthesis, low cost, and non-toxicity. In the study, magnetite (Fe₃O₄) nanoparticles were prepared, coated with glutaraldehyde, characterization processes were performed with Fourier transform infrared spectroscopy (FT-IR), X-ray diffraction pattern (XRD), and Conventional transmission electron microscopy (C-TEM) methods, and idarubicin (IDA) was bound. The cytotoxic effects of idarubicin-bound MNP-GA and free idarubicin on HL-60 cell lines were determined by MTT and ATP tests, and IC₅₀ values were calculated. Flow cytometry was used to evaluate apoptosis status, and the expression of MDR1, Puma, NOXA, BAX, Survivin, and BCL-2 genes were measured by the polymerase chain reaction (PCR). It was found that the IC₅₀ decreased between 5 and 7 times with the use of MNP. In PCR tests, the expressions of apoptotic genes increased, while the expressions of MDR1 and anti-apoptotic genes were decreased in the use of MNP. Apoptosis was found to be increased in flow cytometry measurements. The use of MNP systems has reduced drug resistance since it provides controlled release of the drug and prevents its exit from the cell due to its structure.

Keywords: Acute promyelocytic leukemia, glutaraldehyde, HL-60 cell line, idarubicin, magnetic nanoparticles.

Glutaraldehit kaplı manyetik nanopartiküle idarubisin tutturulması ve HL-60 hücre hattında etkisinin incelenmesi

ÖZ

İdarubisin, meme kanseri ve akut lösemi tedavisinde sıklıkla kullanılan kemoterapötik bir ilaçtır. Bu çalışmada, yüksek stabilite ve düşük toksisiteye sahip bir ilaç hazırlamak için idarubisini glutaraldehit (GA) kaplı manyetik nanopartiküllere (MNP-GA) immobilize edilmesi amaçlanmıştır. Manyetik nanopartiküller kolay sentez edilmesi, düşük maliyetli olması ve toksik olmamasından dolayı tercih edilmiştir. Çalışmada magnetit (Fe₃O₄) nanoparçacıkları hazırlanmış, glutaraldehit ile kaplanmış, Fourier transform kızılötesi spektroskopisi, X-ışını kırınım deseni ve Konvansiyonel transmisyon elektron mikroskobu yöntemleri ile karakterizasyon işlemleri yapılmış ve idarubisin bağlanmıştır. İdarubisine bağlı MNP-GA ve serbest idarubisinin HL-60 hücre hatları üzerindeki sitotoksik etkileri MTT ve ATP testleri ile belirlendi ve IC₅₀ değerleri hesaplandı. Apoptoz durumu flow sitometri ile değerlendirildi ve MDR1, Puma, NOXA, BAX, Survivin ve BCL-2 genlerinin ekspresyonu polimeraz zincir reaksiyonu (PCR) yöntemi ile ölçüldü. MNP kullanımı ile IC₅₀'nin 5 ile 7 kat arasında azaldığı tespit edilmiştir. PCR testlerinde apoptotik genlerin ekspresyonları artarken, MNP kullanımında MDR1 ve anti-apoptotik genlerin ekspresyonları azaldı. Akım sitometri ölçümlerinde apoptoz artışı saptandı. MNP sistemlerinin kullanımı, ilacın kontrollü salınımını sağladığı ve yapısı gereği hücreden çıkışını engellediği için ilaç direncini azaltmıştır.

Anahtar Kelimeler: Akut promyelositik lösemi, glutaraldehit, HL-60 hücre hattı, idarubisin, manyetik nanopartiküller.

1. INTRODUCTION

In recent years, magnetic nanoparticles have significant great attention due to their critical applications in catalysis, biocatalysis, biomedicine, biosensor, bio-separation, and magnetic resonance imaging contrast enhancement.¹⁻³ Magnetic nanoparticles (MNPs) are attractive supports for these areas because of their high surface area/volume ratio and ease of preparation. Magnetic nanoparticles have enormous advantages because they can be easily separated from the reaction medium due to their magnetic properties and are homogeneously dispersed in the solution. In addition, changing the surfaces and polarities of MNPs with chemicals increases their resistance to solutions. Surface modification can be carried out by numerous methods, such as hydrolysis techniques, surfactant-free sonochemical reactions, and sol-gel methods.⁴⁻⁶ During or following their syntheses, coating agents such as oleic acid, epoxy-thiol group, chitosan, and polymers are used for surface modification.⁷⁻¹⁰ In particular, aldehyde groups are used as a binding agent to bind the biomolecule to the support in immobilization applications. Aldehydes are biocompatible molecules and form Schiff bases by binding to amine groups over a wide pH range.

Cancer is defined as reducing or damaging cellular control and normal maturation mechanisms. Its characteristics include heavy cell growth and the ability to spread and metastasize to undifferentiated cells and tissues and adjacent tissues.¹¹ Cancer-related deaths are the second most common disease after cardiovascular diseases globally and in our country in the last 20 years.¹² It is a social problem due to its high prevalence and high risk of death. Many methods, such as surgery, chemotherapy, immunotherapy, hormone therapy, cell transport therapy, and radiation therapy, are used in cancer treatment, and chemotherapy is one of them.¹²

Anthracyclines are among the most effective anticancer drugs ever developed. Anthracycline's cytotoxicity is generally due to its ability to diffuse across the cell membrane, intercalate between DNA base pairs, and target topoisomerase II.¹³ Doxorubicin is one of the earliest anthracyclines and is widely used to treat leukemia, bladder, Hodgkin's lymphoma, and breast cancers. Idarubicin (IDA) is a synthetic analog of daunorubicin and is often used to treat acute promyelocytic leukemia, acute myeloid leukemia, and chronic lymphocytic leukemia. The absence of the methoxy group in the structure of IDA significantly increases lipophilicity, which accelerates cellular uptake and provides higher DNA binding capacity.¹⁴

Traditional chemotherapy is still questioned due to the lack of therapeutic agents at the tumor site, the inadequacy of chemotherapeutic drugs in aqueous media,

rapid clearance, and the lack of cancerous site-selective drugs.¹⁵ The nanoparticle-supported drug is one of the methods that can use as an alternative to chemotherapy. The primary purpose of this method is to increase the effectiveness of chemotherapeutic drugs and minimize the interaction with healthy cells and the side effects of these drugs.

The basic properties of nanoparticles in biotechnology are their nanoscale structure, magnetic properties, and ability to transport active biomolecules in specific tasks. A magnetic nanoparticle consists of a magnetic core, a protective layer, and an organic crosslinking.¹⁶ Glutaraldehyde is the most practical and widely used cross-linker in nanoparticle studies.¹⁷ Sahin et al. attached glutaraldehyde to polyvinyl alcohol-coated MNPs.¹⁸ Zhao et al. bound albumin to amino acid-coated MNPs with the help of glutaraldehyde.¹⁹ In cases where the magnetic nanoparticle is covered with a protective coating material, and an intermediate arm is attached, the particle size becomes larger than desired. So, it makes MNP challenging to enter the cell. In this study, we used glutaraldehyde directly, as a protective coating and cross-linker, without using a protective layer. In this way, the design of nanoparticles has been reduced one step, and the cost has also decreased. The use of glutaraldehyde as a cross-linker and a coating material was applied for the first time in our study. In this respect, our work has been innovative and original, and it is different from other publications using glutaraldehyde-coated nanoparticles.

For this purpose, in this research, magnetite (Fe_3O_4) magnetic nanoparticles were synthesized and coated with glutaraldehyde and finally, IDA was bound. The cytotoxic effect of this complex was investigated on acute promyelocytic leukemia (HL-60) cell line by cell viability analysis. At IC_{50} concentrations, apoptosis status was evaluated by flow cytometry, and expression of MDR1, Puma, NOXA, BAX, Survivin, and BCL-2 genes was measured by polymerase chain reaction (PCR) method.

2. MATERIALS AND METHODS

2.1. Reagents and chemicals

Ferrous sulfate ($\text{FeSO}_4 \cdot 7\text{H}_2\text{O}$, >99%), ferric chloride ($\text{FeCl}_3 \cdot 6\text{H}_2\text{O}$, 97%), glutaraldehyde, dimethyl sulfoxide (DMSO), sodium hydroxide, and phosphate buffer saline (PBS) were purchased from Sigma-Aldrich. All materials were used without further purification. Gaziantep University Medical Biochemistry Department provided an HL-60 cell line. RPMI 1640 medium and fetal bovine serum were purchased from Capricorn. The spectroscopic techniques listed below characterized the magnetic nanoparticles and compared them with the reported characterizations of similar compounds. Fourier transform infrared spectra of materials were recorded

on a Thermo Fourier transform infrared spectroscopy (FT-IR) spectrophotometer; Smart ITR diamond attenuated total reflection (ATR). Elemental analyses (C, N, H) were recorded on a Thermo Scientific Flash 2000, CHNS elemental analyses apparatus. Electronic spectra were obtained on a Perkin Elmer Lambda 25 UV spectrometer. Conventional transmission electron microscopy (C-TEM) spectra were recorded on FEI Tecnai G² Spirit BioTwin CTEM, 20-120 kv (contrast transmission electron microscopy). X-ray diffraction (XRD) patterns were recorded on Rigaku Miniflex CuK α , $\lambda=0.154\text{nm}$.

2.2. Synthesis of magnetic nanoparticles

Glutaraldehyde-coated magnetic nanoparticles were prepared according to co-precipitation method prepared.⁷ Briefly, a solution of FeSO₄.H₂O (1.25 g, 7.33 mmol) and FeCl₃.6H₂O (2.34 g, 8.6 mmol) in 100 mL of water at 90 °C was stirred with a mechanic stirrer for 30 minutes. Next, 12 mL of 0.1 M NaOH solution was added to this solution dropwise at a vigorous stirrer under N₂ atmosphere, and black magnetic nanoparticles were precipitated. Finally, 12 mL of 0.3 M NaOH solution was added to the mixture, and precipitation was finished. It remained under this condition for 30 minutes and turned reddish-brown. It was allowed to cool to room temperature, and the MNPs were washed several times with deionized water until pH reached 7. FT-IR, XRD, and C-TEM characterization analyzes were performed.

2.3. The coating of magnetic nanoparticles by glutaraldehyde

For surface coating and modification with glutaraldehyde, 1.0 g of MNPs was suspended in 100 mL of distilled water by ultrasonication for 30 minutes.²⁰ Next, 5 g of glutaraldehyde solution (25%, 12.5 mmol the glutaraldehyde/MNP ratio used was determined from the amount of MNP remaining in the water. Glutaraldehyde was added so that as little MNP as possible remained in the water phase.) was added to this mixture under vigorous mechanical stirring. The mixture was stirred and ultrasonicated for 2 hours at room temperature. Over time, a brown foam phase appeared on the mixture. The obtained glutaraldehyde-coated magnetic nanoparticles (MNP-GA) were washed with distilled water and acetone and then dried in an oven at 50 °C. FT-IR, XRD and C-TEM characterization analyzes of these materials were performed.

2.4. Idarubicin immobilization

Prepared MNP-GA material was weighed per well with the final concentration of 2 mg/mL and added to a 24-well plate. IDA solutions have dissolved in

DMSO at different concentrations (10.0; 5.0; 1.0; 0.5; 0.1 and 0.01 μM). Samples for each concentration were prepared in triplicate, and the results were averaged. Besides, only MNP-GA and PBS were placed in three wells to observe the toxic effect of synthesized supports. Initially, the absorbance of each IDA solution was measured at a wavelength of 412 nm in a UV-Vis Spectrophotometer (BioTek, Synergy H1 microplate reader) to calculate the percent IDA retention. The prepared plates were mixed horizontally at 600 rpm for 24 hours. After 24 hours, unbound IDA was separated by magnetic decantation, absorbance was measured at 412 nm wavelength, and the percent retention of IDA was calculated. Finally, it was washed two times with PBS solution to remove impurities of usable purity in the cell culture.

2.5. Investigation of cytotoxic effect of MNP-GA-IDA complex on HL60 cell Line

Firstly, the cell number was optimized according to the cells' incubation time and proliferation potential. 1000 μL of HL60 cell suspension was added to the MNP-GA-IDA complex prepared with $1.0\text{-}1.5 \times 10^5$ cells per well.

To compare the prepared drug with free IDA, 900 μL HL60 cell suspensions were added to 24-well microplates with $1.0\text{-}1.5 \times 10^5$ cells per well. 100 μL of IDA was added to the cell suspensions at a final concentration of 10.0; 5.0; 1.0; 0.5; 0.1 and 0.01 μM . Each prepared sample was applied in 3 replicates. In addition, the only cell suspension was added to three wells as the negative control, and MNP-GA without IDA was added to investigate the toxic effect of MNP-GA. Three plates were prepared for the incubation period of 24, 48, and 72 hours. The same procedure was performed twice, one for MTT cytotoxicity analysis and the other for ATP cell viability assay analysis.

2.6. MTT cytotoxicity analysis

MTT viability assay was used to determine cell viability in HL-60 cells. Prepared plates were incubated at 37 °C for 24, 48, and 72 hours in a carbon dioxide incubator. After incubation, 5 mg/mL MTT solution was added to all wells and incubated for 4 hours. Then, the cell culture medium in the wells was carefully removed and 1000 μL of DMSO was added to each well and mixed for 10 minutes to dissolve the violet crystals.

The intensity of the purple color formed during MTT analysis is directly related to cell viability. The absorbance of the plates was measured using a plate reader set to 570 nm. The viability of the cells used as a negative control was considered 100 % and the percentage of viability of the drug-treated cells was

calculated. Consequently, the IC_{50} concentration was calculated from the concentration-dependent curve of cell proliferation.

2.7. ATP cell viability analysis

The CellTiter-Glo Luminescent Cell Viability Assay was utilized to determine cell viability in HL-60 cells. Cells were treated with different concentrations of MNP-GA-IDA complex and free IDA. After 24 h, 48 h, and 72 h incubation at 37 °C, 100 μ L of assay reagent was added to each well. It was incubated on an orbital shaker for 2 minutes to induce cell lysis. The luminescent signals were determined by a luminometer (Synergy H1 Multi-Mode Reader, BioTek Instruments; Winooski, VT, USA). IC_{50} values of incubation times (24, 48, and 72 h) were calculated separately for complex and free IDA. All experiments were repeated three times.

2.8. Determination of apoptotic cells by flow cytometry method

Annexin V is a member of the annexin family of intracellular proteins that bind to phosphatidylserine (PS) in a calcium-dependent manner. PS is typically found in the portions of the plasma membrane facing the cytoplasm- in healthy cells. However, during early apoptosis, the membrane asymmetry is lost, and PS migrates to the outer portions. The fluorochrome-labeled Annexin V can then target and identify apoptotic cells specifically. IC_{50} values obtained from MTT and ATP cytotoxicity tests were used to measure the level of apoptosis. Commercial Annexin V Apoptosis Kit (Biolegend 640932, USA) containing Annexin V and Propidium Iodide (PI) dyes was used to detect apoptosis for MNP-GA-IDA and free IDA.

2.9. Measuring gene expressions

In this study, to examine the effect of magnetic nanoparticles, the expressions of multidrug resistance 1 gene (MDR1), the expressions of apoptotic (Puma, NOXA, and BAX) and anti-apoptotic (Survivin and BCL-2) genes, and β -actin gene as control were measured by PCR method.

Solutions corresponding to the IC_{50} values found in MTT and ATP cytotoxicity tests for MNP-GA-IDA and free IDA were prepared and added to the wells to measure gene expressions. 1×10^5 cells of HL-60 were added to each well and subjected to incubation times of 24, 48, and 72 hours. At the end of the incubation period, the liquid portion of each well was removed and centrifuged at 10000 g for 15 minutes. Then, RNA isolation (Macharey-Nagel NucleoSpin®RNA, 740955.50, Germany), cDNA synthesis from mRNA (Thermo Fischer Scientific, High-Capacity cDNA

Reverse Transcription Kit, Cat No: 4374966, USA), and measurement of gene expressions (Go Taq qPCR® Master Mix, ProMega, USA) by Real-Time PCR (QIAGEN, Germany) was performed according to commercial kit protocols.

3. RESULTS AND DISCUSSION

3.1. Characterization of modified magnetic nanoparticles

Various solvents such as water, ethanol, methanol, and acetone were tried as solvents during the coating of MNPs with glutaraldehyde. However, when organic solvents were used, it was observed that the glutaraldehyde coating was less than water and could not be identified in the characterization. On the other hand, in the experiments where water was used as a solvent, it was observed that the coating was achieved when the foam formed on the surface of the mixture was separated and analyzed after a while.

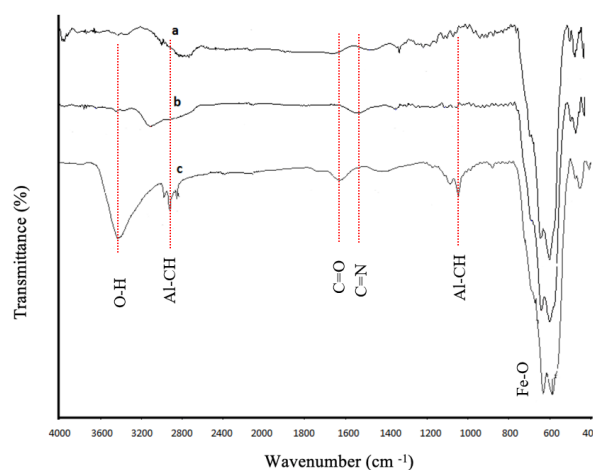


Figure 1. FT-IR spectra of (a): MNPs, (b): MNP-GA, and (c): MNP-GA-IDA.

The characterization of magnetic nanomaterials was verified by FT-IR, C-TEM), XRD, ICP-OES, and UV-Vis. **Figure 1** shows the FT-IR spectra of MNPs (a), MNP-GA (b), and MNP-GA-IDA (c). The characteristic peak for Fe-O was observed at 541 cm^{-1} for two materials. A strong O-H band about 3400-3450 cm^{-1} was observed in both MNP-GA and MNP-GA-IDA, indicating that -OH groups cover the surface of Fe_3O_4 nanoparticles. The intensity of this bond increased after immobilization due to the presence of -OH groups in hemoglobin. C-H aliphatic bands of IDA were observed at 2900 and 1051 cm^{-1} . The peaks observed at 1633 cm^{-1} indicate the presence of C=O bands of the aldehyde group of IDA and glutaraldehyde. C=N band observed at 1524 cm^{-1} refers to the Schiff base formed between hemoglobin and MNP-GA.⁹

Figure 2 shows the XRD patterns of MNPs (a) and MNP-GA (b) nanocomposites. Fe₃O₄ characteristic peaks were observed for both samples with the indices ((220), (311), (400), (422), (511), and (440)). These peaks refer to spinel structure (JCPDS card number is 65-3107). The primary diameter of the magnetic nanoparticles was calculated as 20 nm and 24.8 nm for MNPs and MNP-GA, respectively, using the peak of (311) from the Scherrer formula. These data show that the surface modification did not change the crystal structure and size of Fe₃O₄, suggesting that the immobilization occurred only on the particle surface.

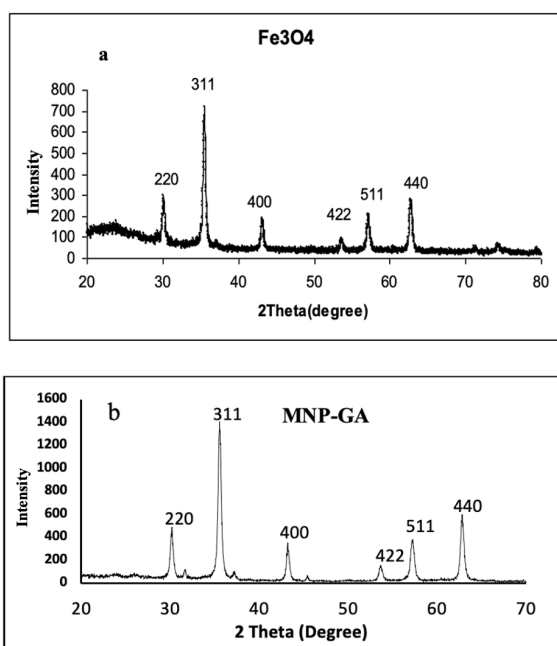


Figure 2. XRD spectra of (a): Magnetic Nanoparticles, (b): Magnetic Nanoparticles-Glutaraldehyde.

Contrast transmission electron microscopy images of MNP, MNP-GA, and MNP-GA-IDA are shown in Figure 3. The dark black colored spots in the middle indicated the magnetic nanoparticles, and the lighter outer image indicated the coated organic material. Most nanoparticles are spherical, and the average particle size was calculated as 21.0±2.5 nm (200 counted particles), 23.8±3.1 nm (364 counted particles), and 30.8±6.0 (172 counted particles) for MNPs, MNP-GA, MNP-GA-IDA, respectively. It is clear that MNP-GA does not agglomerate and is well-dispersed, meaning that the glutaraldehyde coating prevents the agglomeration of particles. The C-TEM image of MNP-GA-IDA shows that the coating thickness is 2-6 nm, and there are two layers on the surface of spherical-shaped magnetic nanoparticles. The first of these layers is glutaraldehyde, while the other layer shows IDA. When the MNP-GA and MNP-GA-IDA images are compared, surface difference is remarkable. It can be seen from the C-TEM images that the IDA is attached to the support

material. It was observed that the agglomeration amount of the particles increased after the IDA coating. According to all analysis results, it was understood that MNP was synthesized correctly and in desired sizes.

Table 1. Atomic composition of nanomaterials.

Material	Fe %	O %	C %	% N
MNP	72.36	27.64	-	-
MNP-GA	69.42	25.92	1.96	-
MNP-GA-IDA	66.32	27.84	3.27	2.57

C: Carbon, Fe: Iron, GA: Glutaraldehyde, IDA: Idarubicin, MNP: Magnetic nanoparticles, N: Nitrogen, O: Oxygen,

The atomic composition of the prepared nanomaterials is given in Table 1. According to the ICP-OES results, the amount of Fe atoms in MNP-GA-IDA decreases compared to MNPs while the amount of C atoms increases. Although MNP and MNP-GA materials do not contain nitrogen atoms, MNP-GA-IDA obtained by binding IDA is expected to contain nitrogen. Energy-dispersive X-ray spectroscopy analysis showed that the nitrogen content was 2.57%. The increase in carbon and nitrogen amounts when the iron level decreases indicate that glutaraldehyde is coated on the MNP surface, and IDA is immobilized to MNP-GA.

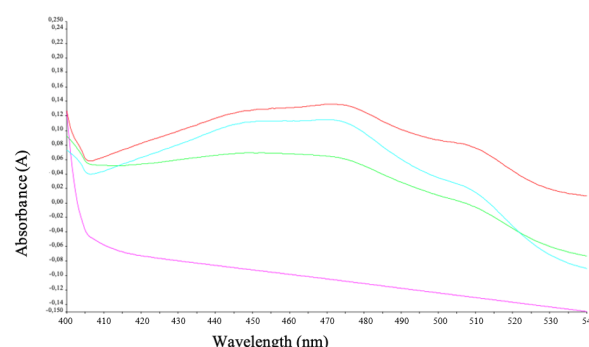


Figure 4. UV-Vis spectra of IDA. Red peak freshly prepared idarubicin solution, the blue curve is MNP-free IDA solution prepared in PBS and subjected to the same procedures as in the idarubicin binding assays, green curve remaining solution from MNP-GA binding and the purple curve represents the absorption spectra of the PBS solution.

The UV-Vis spectrum is shown in Figure 4. Red peak freshly prepared IDA solution, the blue curve is MNP-free IDA solution prepared in PBS and subjected to the same procedures as in the IDA binding assays, the green curve remaining solution from MNP-GA binding, and the purple curve represents the absorption spectra of the PBS solution. When the spectra were compared, IDA alone degraded at room temperature as expected. The decrease in peak intensity indicates the immobilization of IDA to MNP-GA. Two characteristic peaks appear at 447 nm and 471 nm from the UV-Vis spectrum of MNP-GA-IDA,

indicating that IDA retains its structure after immobilization. The wavelength at which substances absorb is in the blue region. The complementary color of blue is orange. The color of the idarubicin solution is also orange. In this region, $n-\pi^*$ and $\pi-\pi$ transitions are seen. These transitions are due to the benzene ring in idarubicin.²¹ Evidence of the stability of the glutaraldehyde-coated MNP material is given in Figure 4. Accordingly, the absence of peaks of pure GA in the presence of MNP-GA indicates that GA remains on the MNP surface.²²

Coating with glutaraldehyde was performed to maintain the magnetic nanoparticles' stability, prevent agglomeration and bind the drug. Glutaraldehyde is an aldehyde containing a carbonyl group at both ends. This way, one terminal can be connected to the magnetic nanoparticle, while the other terminal can be connected to IDA by forming a Schiff base. C-TEM images show that agglomeration is low, and aspherical grain structure is formed (Figure 3).

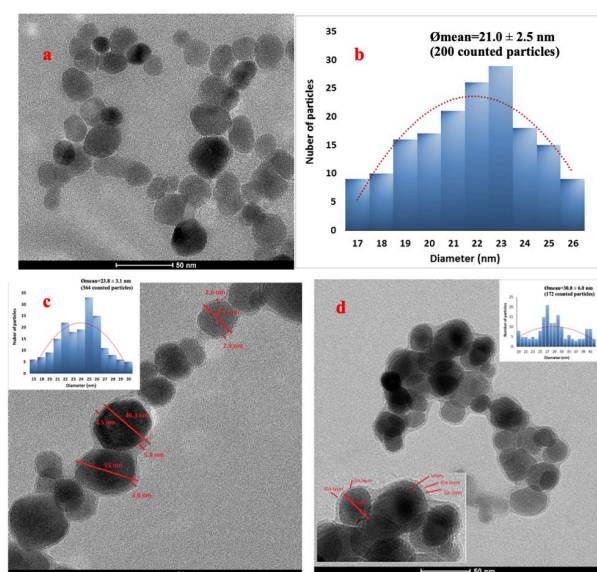


Figure 3. (a): C-TEM image of MNPs, (b): particle size distribution of MNPs, (c): C-TEM image and particle size distribution of MNP-GA, and (d): C-TEM image and particle size distribution of MNP-GA-IDA.

IDA was attached to the magnetic nanoparticles for which characterization processes were performed. IDA-linked constructs were checked by FT-IR analysis. The characteristic C=N stretching peaks seen in the FT-IR spectrum indicate binding of the IDA (Figure 1).

3.2. Cytotoxicity analysis findings

MTT assay was performed to determine the cytotoxic effects of different concentrations of free IDA and MNP-GA-IDA on the HL60 acute promyelocytic leukemia cell line. From the concentration-dependent cell proliferation

curve, the concentration at which 50% of the cells were viable (IC_{50}) was calculated from the data obtained from the MTT assay. Living cells reduce tetrazolium to purple-colored formazan crystals by mitochondrial reductase activity. First, DMSO is added to dissolve the formazan crystals in the reaction medium, and then the viability analysis is completed by measuring the optical density of the chromogen at 570 nm. According to the result obtained from the analysis, a positive correlation was observed between the amount of absorbance and the number of viable cells. The IC_{50} values of both the IDA and MNP-GA-IDA complex calculated at 24, 48 and 72 hours from the MTT test are given in Table 2.

Table 2. IC_{50} values of MNP-GA-IDA and free idarubicin in the HL-60 cell line

		IC_{50} (μ M)		
		24 h	48 h	72 h
		(mean \pm SD)	(mean \pm SD)	(mean \pm SD)
IDA	MTT	3,106 \pm 0.179	0,834 \pm 0.061	0,319 \pm 0.035
	ATP	3,303 \pm 0.148	0,819 \pm 0.015	0,298 \pm 0.059
MNP-GA-IDA	MTT	0,439 \pm 0.054	0,094 \pm 0.012	0,076 \pm 0.010
	ATP	0,441 \pm 0.057	0,098 \pm 0.019	0,068 \pm 0.007

GA: Glutaraldehyde, IDA: Idarubicin, MNP: Magnetic nanoparticles

The basic principle of luminescence ATP cell viability test; recombinant luciferase enzyme oxidizes luciferin to oxyluciferin in the presence of ATP and molecular oxygen. At the same time, the luminescence radiation level and the amount of ATP are parallel. Therefore, as cytotoxicity increases in the ATP cell viability test, the luminescent radiation decreases, and the measured optical density decreases. The luminescence ATP cell viability assay was used to calculate the concentration (IC_{50}) at which 50% of the cells were viable from the concentration-dependent cell proliferation curve. The IC_{50} values of both the IDA and MNP-GA-IDA complex calculated at 24, 48 and 72 hours from the ATP test are given in Table 2. When the results were examined, it was determined that the IC_{50} values in the MNP-GA-IDA complex were between 5 and 8 times lower than in the free IDA application.

3.3. Apoptosis findings

Apoptotic cells are divided into early and late apoptotic cells. In cases where the cell membrane remains intact and only PS is released, it is classified as an early apoptotic cell, and when the plasma membrane becomes permeable, it is classified as a late apoptotic cell, known as secondary necrotic. The direct exposure of healthy living cells to trauma, such as extreme heat, mechanical and chemical attacks, and exposure to excessive toxic drugs, cause necrotic cell formation as the membrane completely breaks down.²³ A flow cytometry device determined apoptosis status for MNP-GA-IDA and free IDA. In Figure 5, the LL region represents viable cells, the UL and UR regions represent apoptotic cells, and the LR region represents necrotic cells. In the development of an effective drug, the cells should be recruited at

apoptotic sites. When Figure 5 is examined, it is seen that the control cells are mostly alive. When the MNP-GA-IDA complex is applied, the cells begin to accumulate in the apoptotic regions, and the cells do not go into necrosis. This shows that the MNP-GA-IDA complex kills cells not by necrotizing but by stimulating the apoptotic pathway.

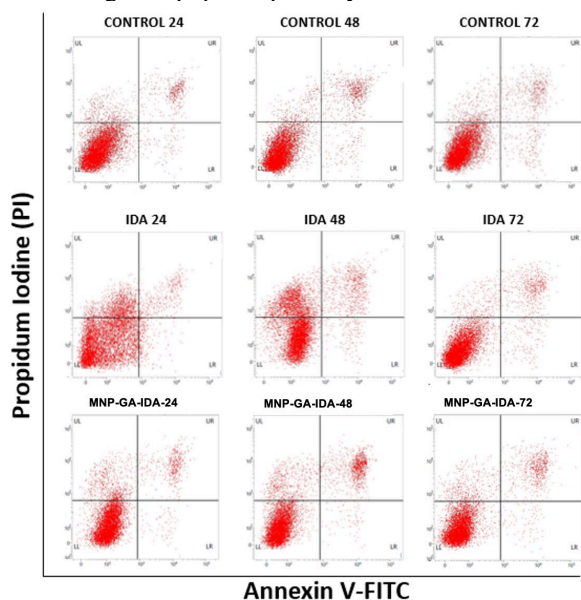


Figure 5. Apoptosis findings of control, idarubicin and Magnetic Nanoparticles-Glutaraldehyde-idarubicin (LL: Live cell, UL: Early apoptotic cell, UR: Late apoptotic cell, LR: Necrotic cell).

3.4. Gene Expressions Findings

To examine changes in cell apoptosis, the expressions of multidrug resistance 1 gene (MDR1) in HL-60 cell line, apoptotic (Puma, NOXA, and BAX) and anti-apoptotic (Survivin and BCL-2) genes, and β -actin gene as control were measured. Gene expressions were analyzed in duplicate and averaged.

$2^{-\Delta\Delta Ct}$ (coefficient of variation relative to control gene) values for each gene are given in Table 3. Expressions of genes belonging to the control group were accepted as 1. Expressions of genes belonging to MNP-GA-IDA and free IDA groups were given compared to the control group. When the results are examined, it is seen that while the expressions of apoptotic genes increase, the expressions of anti-apoptotic genes decrease in MNP-GA-IDA application. It is also seen that MDR1 expressions are severely decreased. In particular, a 6- and 10-fold increase was observed in apoptotic NOXA gene expressions at the end of 48 and 72 hours, while there was a decrease of more than 50% in the expressions of anti-apoptotic and MDR1 genes. These results show that the drug administered with the nanoparticle complex kills cancerous cells at lower doses by increasing cell apoptosis and reducing multidrug resistance.

In this study, magnetic nanoparticles were used to prevent the development of multidrug resistance and reduce the toxic effect of IDA on healthy tissues by reducing the effective dose.

The cytotoxic effects of magnetic nanoparticles loaded with IDA on the HL-60 cell line were investigated. When the results obtained from MTT and ATP cytotoxicity tests are examined (Table 2), it is seen that the IC_{50} values in the IDA immobilized MNP-GA structure is decreased compared to pure IDA. A decrease in the effective dose (IC_{50}) indicates an increase in the cytotoxic effect. These results show that the synthesized IDA-loaded magnetic nanoparticles increased the cytotoxic effect. The primary purpose of this study was to give the patient a lower concentration that would have the same effect due to the toxic effects of the drug given during chemotherapy. There may be many reasons for the decrease in the effective dose of the drug. These; maybe because the magnetic nanoparticle facilitated the drug uptake into the cell, increased the stability of the drug, increased the half-life with the gradual release of the drug, and decreased drug resistance. There are no magnetic nanoparticle studies in the literature to reduce the effective dose of IDA in the HL-60 cell line. When studies with different drugs or cells are examined, Gunduz et al. attached IDA to nanoparticles coated with polyethylene glycol. They found IC_{50} values two times lower than free IDA in the MCF-7 cell line.¹⁵

Our study found that MDR1 gene expressions in the MNP-GA-IDA system were decreased compared to the free IDA molecule. Thus the drug resistance in the cell decreased, and the drug became more effective than the free IDA molecule. In their study, Cheng et al. found that drug resistance decreased in the use of drugs loaded with magnetic nanoparticles in resistant K562 cells.²⁴ In addition, Zhao et al. found that the using magnetic chitosan nanoparticles in glioblastoma cell lines downregulated MDR1 gene expressions.²⁵

On the other hand, magnetic nanoparticles enter the cell by endocytosis due to their size.²⁶ Gupta et al. stated that the ideal particle size for drug delivery should be between 10-100 nm. In this way, the drug will be freed from being catabolized by the reticuloendothelial system (RES).²⁷ In the XRD and C-TEM analyses performed in this study, particle sizes were smaller than 50 nm. In this way, our drug-loaded magnetic nanoparticles can remain in the cell. Furthermore, nanoparticles entering the cell provide a gradual release of the drug. In this way, it is ensured that the drug has a continuous cytotoxic effect in the cell. Furthermore, as the gradual release of the drug by the MNP enables the drug to get rid of P-

glycoprotein-mediated drug pumps, drug resistance in the cell also decreases.²⁶

Table 3. $2^{-\Delta\Delta Ct}$ values of genes.

		PUMA (mean \pm SD)	BAX (mean \pm SD)	NOXA (mean \pm SD)	Survivin (mean \pm SD)	BCL-2 (mean \pm SD)	MDR1 (mean \pm SD)
Control	24h	1,00	1,00	1,00	1,00	1,00	1,00
	48h	1,00	1,00	1,00	1,00	1,00	1,00
	72h	1,00	1,00	1,00	1,00	1,00	1,00
IDA	24h	0,80 \pm 0,10	0,99 \pm 0,11	1,34 \pm 0,21	0,91 \pm 0,08	0,53 \pm 0,10	0,81 \pm 0,08
	48h	0,89 \pm 0,09	3,23 \pm 0,45	1,92 \pm 0,18	0,90 \pm 0,14	0,75 \pm 0,09	0,61 \pm 0,03
	72h	1,32 \pm 0,08	2,09 \pm 0,18	2,07 \pm 0,24	0,95 \pm 0,11	0,74 \pm 0,05	0,71 \pm 0,06
MNP- GA- IDA	24h	1,93 \pm 0,32	1,15 \pm 0,09	2,88 \pm 0,46	0,56 \pm 0,07	0,65 \pm 0,08	0,62 \pm 0,04
	48h	1,46 \pm 0,22	2,22 \pm 0,31	6,08 \pm 0,54	0,55 \pm 0,08	0,92 \pm 0,12	0,55 \pm 0,08
	72h	1,39 \pm 0,24	4,48 \pm 0,72	10,85 \pm 1,23	0,51 \pm 0,04	0,61 \pm 0,06	0,41 \pm 0,06

GA: Glutaraldehyde, IDA: Idarubicin, MNP: Magnetic nanoparticles,

When the multi-drug resistance gene expressions are examined (Table 3), it is seen that the expressions in MNP structures are decreased compared to the control cells. These findings support the cytotoxicity findings and show that IDA-loaded MNP structures reduce drug resistance. Decreased drug resistance allows the drug to act at lower concentrations.

One of the reasons for the development of drug resistance is the disruption of the apoptosis mechanism. Apoptosis is regular and tightly controlled programmed cell death. The molecular mechanism of drug-induced apoptosis is associated with a mitochondrial dysfunction characterized by increased mitochondrial membrane permeability and the release of cytochrome C from the mitochondria.²⁸ When the expressions of apoptotic and anti-apoptotic genes were examined, it was found that the expressions of apoptotic genes increased, and the expressions of anti-apoptotic genes decreased (Table 3).

When the flow cytometry results were examined (Figure 5), it was observed that MNP-GA loaded with IDA did not lead to necrosis of the cells in 24, 48, and 72 hours incubations. Our results show that our MNP systems do not cause necrotic effects. Therefore, it is desired that the drug selected as a cancer drug has an apoptotic effect on the cell. Especially drugs that lead the cell to late apoptosis are preferred because they kill the cell gradually.

In summary, our results show that the use of nanoparticle structure significantly reduces the effective dose of the drug. It was seen that the MNP-GA-IDA structure was most effective at the 72nd hour, according to all results. Further, it was observed

that the expressions of MDR1 and anti-apoptotic genes decreased, and the expressions of apoptotic

genes increased despite the use of lower doses of drugs. In addition, it was seen from the Annexin V results that the MNP structure was not necrotic. Therefore, reducing the drug dose will reduce the patient's drug exposure, thus reducing the side effects. In addition, reducing the use of drugs will provide significant economic savings.

Considering all these results, it is seen that MNP drug delivery systems have many advantages over free drugs. These; (i) Free drugs between 10-100 nm are eliminated and excreted due to their small size, while drug-loaded MNPs can remain in circulation due to their size around 20-50 nm,²⁹ (ii) since drug-loaded MNP has lower IC₅₀ values than free drug, side effects may decrease²⁹ (iii) drug-loaded MNPs can quickly enter vessels and are easily targeted to cancer cells³⁰ (iv) since drugs bind to MNPs, they are less affected by environmental conditions and have higher stability than free drug.³⁰

4. CONCLUSIONS

In the present research, idarubicin was successfully immobilized after Fe₃O₄ magnetic nanoparticles were prepared using the precipitation method, and then coated with glutaraldehyde. It is clear that the nanoparticle has been synthesized and has the desired dimensions from the FT-IR, XRD, and C-TEM testing results. The MNP-GA-IDA complex was administered to HL-60 cells, and the change in cytotoxicity against free idarubicin was measured using MTT and ATP assays. Idarubicin complexed with the nanoparticle had 5 to 7 times lower IC₅₀ values. Furthermore, it was demonstrated that the MNP-GA-IDA complex increased the expression of

apoptotic genes compared to free idarubicin and decreased the expressions of anti-apoptotic genes and the MDR1 gene. Consequently, it has been ascertained that the utilization of MNP systems decreases the effective dose of the drug, stimulates apoptosis, and reduces the prevalence of resistance to multiple drugs. Since our study is the first magnetic nanoparticle study to reduce the effective dose of IDA in the HL-60 cell line and the first study to directly link drugs with GA, a cross-linker, without using any organic preservatives, it will be a reference and guide for future research.

ACKNOWLEDGEMENTS

Dr. Hasan Ulusal has received research grants from the Scientific and Technological Research Council of Türkiye (TÜBİTAK) (BİDEB 2211-E domestic graduate scholarship program). Dr. Fatma Ulusal has received research grants from TÜBİTAK (BİDEB 2218 postdoctoral research fellowship program). This study was funded by the Management Unit of Scientific Research Projects of Gaziantep University (BAP project no: TF.DT.19.54 and TF.19.52). These are gratefully acknowledged.

Conflict of interests

The authors declare that there is no conflict of interest.

REFERENCES

- Chawla, S.; Pundir, C. S. *Biosens Bioelectron* **2011**, 26 (8), 3438-3443.
- Luo, S.; Zheng, X.; Xu, H.; Mi, X.; Zhang, L.; Cheng, J.-P. *Adv Synth Catal* **2007**, 349 (16), 2431-2434.
- Zheng, M.; Zhang, S.; Ma, G.; Wang, P. *J Biotechnol* **2011**, 154 (4), 274-280.
- Ghanbari, D.; Salavati-Niasari, M.; Ghasemi-Kooch, M. *J Ind Eng Chem* **2014**, 20 (6), 3970-3974.
- Lu, Y.; Yin, Y.; Mayers, B. T.; Xia, Y. *Nano Lett* **2002**, 2 (3), 183-186.
- Waseem, M.; Munsif, S.; Rashid, U.; Imad ud, D. *Appl Nanosci* **2014**, 4 (5), 643-648.
- Jadhav, N. V.; Prasad, A. I.; Kumar, A.; Mishra, R.; Dhara, S.; Babu, K. R.; Prajapat, C. L.; Misra, N. L.; Ningthoujam, R. S.; Pandey, B. N.; Vatsa, R. K. *Colloids Surf B Biointerfaces* **2013**, 108, 158-168.
- Mahmood, I.; Ahmad, I.; Chen, G.; Huizhou, L. *Biochem Eng J* **2013**, 73, 72-79.
- Tang, T.; Fan, H.; Ai, S.; Han, R.; Qiu, Y. *Chemosphere* **2011**, 83 (3), 255-264.
- Zhou, H.; Li, W.; Shou, Q.; Gao, H.; Xu, P.; Deng, F.; Liu, H. *Chinese J Chem Eng* **2012**, 20 (1), 146-151.
- Lubbe, A. S.; Alexiou, C.; Bergemann, C. *J Surg Res* **2001**, 95 (2), 200-6.
- Ferlay, J.; Soerjomataram, I.; Dikshit, R.; Eser, S.; Mathers, C.; Rebelo, M.; Parkin, D. M.; Forman, D.; Bray, F. *Int J Cancer* **2015**, 136 (5), E359-86.
- Ma, P.; Dong, X.; Swadley, C. L.; Gupte, A.; Leggas, M.; Ledebur, H. C.; Mumper, R. J. *J Biomed Nanotechnol* **2009**, 5 (2), 151-61.
- Ma, P.; Mumper, R. J. *Nano Today* **2013**, 8 (3), 313-331.
- Gunduz, U.; Keskin, T.; Tansik, G.; Mutlu, P.; Yalcin, S.; Unsoy, G.; Yakar, A.; Khodadust, R.; Gunduz, G. *Biomed Pharmacother* **2014**, 68 (6), 729-36.
- McBain, S. C.; Yiu, H. H.; Dobson, J. *Int J Nanomedicine* **2008**, 3 (2), 169-80.
- Pinto, R. V.; Gomes, P. S.; Fernandes, M. H.; Costa, M. E. V.; Almeida, M. M. *Mater Sci Eng C Mater Biol Appl* **2020**, 109, 110557.
- Sahin, S.; Ozmen, I. *J Pharm Biomed Anal* **2020**, 184, 113195.
- Zhao, L.; Yang, B.; Dai, X.; Wang, X.; Gao, F.; Zhang, X.; Tang, J. *J Nanosci Nanotechnol* **2010**, 10 (11), 7117-20.
- Danafar, H.; Sharafi, A.; Askarlou, S.; Manjili, H. K. *Drug Res (Stuttg)* **2017**, 67 (12), 698-704.
- Barbey, C.; Bouchemal, N.; Retailleau, P.; Dupont, N.; Spadavecchia, J. *ACS Omega* **2021**, 6 (2), 1235-1245.
- Matei, A.; Puscas, C.; Patrascu, I.; Lehene, M.; Ziebro, J.; Scurtu, F.; Baia, M.; Porumb, D.; Totos, R.; Silaghi-Dumitrescu, R. *Int J Mol Sci* **2020**, 21 (9).
- Poon, I. K.; Hulett, M. D.; Parish, C. R. *Cell Death Differ* **2010**, 17 (3), 381-97.
- Cheng, J.; Cheng, L.; Chen, B.; Xia, G.; Gao, C.; Song, H.; Bao, W.; Guo, Q.; Zhang, H.; Wang, X. *Int J Nanomedicine* **2012**, 7, 2843-52.
- Zhao, P.; Wang, H.; Gao, H.; Li, C.; Zhang, Y. *Neurol Res* **2013**, 35 (8), 821-8.

26. Fang, C.; Kievit, F. M.; Veisoh, O.; Stephen, Z. R.; Wang, T.; Lee, D.; Ellenbogen, R. G.; Zhang, M. *J Control Release* **2012**, 162 (1), 233-41.
27. Gupta, A. K.; Gupta, M. *Biomaterials* **2005**, 26 (18), 3995-4021.
28. Kim, R.; Emi, M.; Tanabe, K.; Toge, T. *Cancer* **2004**, 101 (11), 2491-502.
29. Attari, E.; Nosrati, H.; Danafar, H.; Kheiri Manjili, H. *J Biomed Mater Res A* **2019**, 107 (11), 2492-2500.
30. Tarantash, M.; Nosrati, H.; Kheiri Manjili, H.; Baradar Khoshfetrat, A. *Drug Dev Ind Pharm* **2018**, 44 (11), 1895-1903.